Analysis of Skin Cancer Using Fuzzy and Wavelet Technique – Review & Proposed New Algorithm

Nilkamal S. Ramteke[#1] and Shweta V. Jain[*2]

[#1]*M.Tech Student and* [#2]*Asst. Professor*

Department of Computer Science and Engineering

Shri Ramdeobaba College of Engineering & Management

Nagpur, INDIA

Abstract **- This paper first reviews the past and present technologies for skin cancer detections along with their relevant tools. Then it goes on discussing briefly about features, advantages or drawbacks of each of them. Then we discuss the mathematics preliminary required to process the image of skin cancer lesion using our proposed scheme. This paper presents a new approach for Skin Cancer detection and analysis from given photograph of patient's cancer affected area, which can be used to automate the diagnosis and theruptic treatment of skin cancer. The proposed scheme is using Wavelet Transformation for image improvement, denoising and Histogram Analysis whereas ABCD rule with good diagnostic accuracy worldwide is used in diagnostic system as a base and finally Fuzzy Inference System for Final decision of skin type based on the pixel color severity for final decision of Benign or Malignant Skin Cancer..**

Keywords **- Skin Cancer, Melanoma, Fuzzy Inference System, Wavelet, Segmentation.**

I. INTRODUCTION

Skin cancer - a malignant tumor that grows in skin cells is one of the most common of all human cancer and in the present-days, accounts for more than 50% of all types of cancers around the world. Skin cancer (also known as "skin neoplasm") is skin's unwanted growth with differing causes and varying degrees of malignancies. It can spread very fast to all organs/parts of human body through lymphatic system or blood. The incidences of "melanoma - the deadliest form of skin cancer has been on rise at an alarming rate of 3% per year [1]. Detection of malignant melanoma in its early stages considerably reduces morbidity and mortality. Skin cancer can be cured at very high rates with simple and economical treatments. For the benefit of human race, there is a need of diagnosis of skin cancer at an early stage and lots of researchers already working in that direction by means of hardware and software development using different techniques. In this regards, we are suppose to use images of cancer affected skin of patients frequently. So the basic aim of this proposed paper is, to have a simple, efficient and automatic skin cancer, detection and diagnosis system with the use of commonly available software for non-experts/clinicians/doctors. This paper proposes on the use of commonly available software - MATLAB®. We are proposing the use of fuzzy logic along with wavelet techniques for the qualitative and quantitative analysis of skin cancer images.

This paper is organized as follows: Work done by different researchers are briefly discussed in Section II. Overview of Skin Cancer & its detection techniques are given in Section III. The common steps of skin cancer image processing along with its different tools and techniques are discussed in Section IV. The Mathematical detail of our proposed image processing algorithms of Computer Aided Diagnosis System is presented in Section V and lastly, we draw some conclusions in Section VI.

II. BACKGROUND WORK

Indira, D.N.V.S.L.S. [2] gives different method to develop texture analysis based classification by applying multi-level wavelet transformation to the given images. Jain, Y. K. [3] focuses on the development a skin cancer screening system that can be used by non-experts to classify normal from abnormal cases, using feature detection and classification techniques. The features are extracted using wavelet transform were as the classification is done using neural networks. Fatima, R. [4] introduces a multi-parameter extraction and classification system to aid an early detection skin cancer melanoma Fassihi, N. [6] utilizes morphologic operators in segmenting a d wavelet analysis to extract the feature which culminated in to better melanoma diagnosis system. Alcon, J. F. [7] has used pigmented skin lesion's images, acquired using consumer digital camera for automatic melanoma diagnosis with an accuracy of 86%, sensitivity of 94% and specificity of 68%. Odeh, S. M. [9] presented a diagnosis system based on Neuro-Fuzzy inference system based algorithm for three different types of skin lesions. Ogorzalek, M. J. [12] proposed computer aided enhanced diagnostic tools for non-standard image decomposition. Blackledge, J.M. [13] uses recognition and classification of digital images with texture based characterization of digital images. He also describes fuzzy logic and membership function theory based decision engine. Patwardhan, S. V. [15] uses wavelet transformation based skin lesion images classification system which utilizes a semantic representation of spatial frequency information contains in the skin lesion images.

So for image processing and analysis different researchers has worked in DIP, Fuzzy logic, neural network, artificial intelligence, wavelet transformation, lesion images segmentation techniques in parts.

We are systematically utilizing their research to detect and analyse skin cancer severity. We are proposing fuzzy logic based cancer severity quantification of skin cancer image. The proposed system will try to overcome different problem cited by above researcher.

III. Skin Cancer - an overview

The skin is the largest organ of the human body as well as our first line of defence. Skin is divided into three layers, viz. epidermis (outer layer), dermis (middle layer) and hypodermis/subcutis (deepest layer) as shown in Fig. 1. The epidermis mainly consists of keratinocytes. It also contains melanocytes, cells responsible for our skin pigmentation, which provides natural protection against sun's rays. They are evenly distributed in the skin along the basal layer at the dermo-epidermal junction. Melanin is the major pigmentation factor for human skin color variation. Below the epidermis is the dermis layer, it contains special cells which repair our skin. The hypodermis is deepest layer mainly made from fat and manages feeding, excreting and heat exchange. Fat manages the insulation and sweat glands from this layer controls heat exchange of human body.

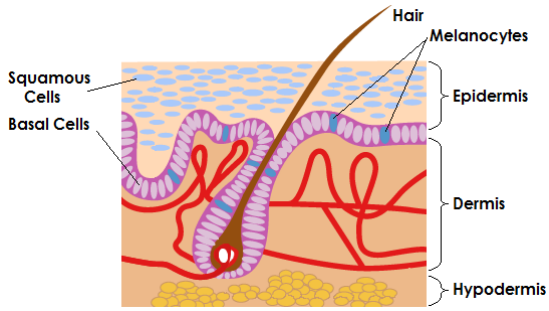

Fig. 1 Illustration of details of Human Skin [www.emedicinehealth.com][17]

Cancer can be defines as a diseases in which there is uncontrollable growth of cells aggressively, invasively and metastatically. Cancer can be classified based on tissues from which the cancerous cell originates. Skin cancer is by far the most common of all cancer and it usually begins with skin lesions. So based on the nature of these skin lesions, skin cancer can be majorly divided into melanoma and non-melanoma. The malignant non-melanoma lesions are further divided into basal cell carcinoma (BCC) and squamous cell carcinoma (SCC)

BCC is the most common type of skin cancer. It originates from the basal keratinocytes of the epidermis. The most common example of such cancer is a pink, pearly papule or plaque all sun -exposed skin. BCC can occur in fair complexion, chronic sun exposure and ionizing radiation. BCC can be seen on the human face, particularly the nose. BCC tends to grow slowly. Proper lighting is most important in detecting BCC at their earliest stages.

SCC is second most common type, arises from the epidermal keratinocytes. The common example of SCC represents a scaly papule, plaque or nodule on sun-exposed skin. In addition to BCC, SCC can occur because of cigarette smoking. The skin of the head and neck are the most common location for SCC. SCC can grow rapidly and has an increased risk of metastasis, especially in chronically immunosuppressed patients, such as organ transplant recipients.

Malignant melanoma, the third most common and the leading cause of death is the second type of skin cancer. Although Melanoma can occur in many organs, the most common form, cutaneous melanoma arises from the melanocytes that are found in basal layer of the epidermis, hair follicles, sebaceous glands and other adnexal structure. Melanoma often presents as an irregularly bordered, pigmented macule. A melanoma presents numerous shades of color, ranging from tan to brown to jet-black, but they also be evenly colored. Papular or nodular lesions are worrisome for deeper, more invasive disease. Melanoma is the leading cause of skin cancer-related deaths and early detection and diagnosis is the need of present day.

Most of the times, the patches of darker color on the skin represents pigmented skin lesions and is the result of excessive melanin concentration. In benign lesions (e.g., common nevi), melanin deposits are normally found in the epidermis. In malignant lesions (i.e., melanoma), the melanocytes reproduce melanin at a high, abnormal rate. Due to the penetration of malignant melanocytes into the dermis, they leave melanin deposits there and thus changing the nature of skin coloration. The presence of melanin in the dermis is the most significant sign of melanoma.

Melanoma typically grows horizontally within the epidermis. It then penetrates into the dermis. Therefore, accurate diagnosis of malignant melanoma at an early stage, leading to earlier treatment is crucial to successful cancer management and is a crucial issue for dermatologists. Earlier detection and therapy also lead to less morbidity and decreased cost of therapy.

The standard method to evaluate a skin growth to rule out melanoma is by biopsy followed by histopathological examination. The challenge lies in identifying the lesions that have the highest probability for being melanoma.

With highly accurate (75%) diagnosis, there is a need to develop efficient schemes for the clinical diagnosis and to support the dermatologists with computer-aided diagnosis (CAD) systems. The main objective of such systems is to

assist the physician in different analysis steps, such as the lesion boundary detection, the quantification of diagnostic features, the classification of lesions, the visualization, the storage, the database management, etc.

During the last three decades, there has been significant evolution in the diagnosis of early melanoma as shown in Table I.

TABLE I
EVOLUTION OF PRIMARY APPROACHES TO MELANOMA DIAGNOSIS [18]

Decades	Input	Examples
Pre 1980s	Gross features	Bleeding, Ulceration
1980	Morphologic clinical features, Screenings	ABCD(E)s, Mass screenings, Public & professional education
1990	Subsurface features	Dermoscopy
2000 Onwards	Digital features, Sub-cellular features	Computer analysis, in-vivo diagnosis

Brief overview of some of the emerging melanoma diagnosis systems/techniques are given in Table II

TABLE II
EMERGING TECHNOLOGIES IN MELANOMA DIAGNOSIS

Diagnosing Technology	Owner	Important Features
Confocal Scanning Laser Microscopy (CSLM)	VivaScope 3000, Lucid, Rochester, NY, USA	It has a flexible hand-held scanner. Its longer wavelengths can measures into papillary dermis. We can use it upto a depth of 300µm. But melanomas without in situ component will likely escape detection. It captures poor resolution patterns.
Electrical Bioimpedance		It completes all process in 7 minutes. But it is also affected by the varying impedance properties of human skin.
MelaFind®	MELA Sciences, Inc., Irvington, NY, USA	This type of digital dermoscope with specialized probe & software to assist and differentiate between melanoma and other skin lesions. It has a hand-held scanner. It creates multispectral sequence of image in less than 3 seconds.
MoleMax™	Derma Medical Systems, Vienna, Austria	This is a computer aided polarized light dermoscope which is used for hand held video dermoscope for close-up imaging. It uses two camera systems for total body photography. But there is no computer diagnostic analysis
Optical Coherence Tomography (OCT)		It captures high resolution images than ultrasound and greater depth than CSLM. Ointment is needed to reduce scattering and increase detection depth.
Spectrophoto-metric Intracutaneous Analysis (SIA)	SIAscope, Astron Clinica, Cambridge, UK	The SIA uses 12 wavebands to evaluate the skin rather than conventional broadband white light. It has a hand-held scanner. It does a diagnosis of lesions less than 2mm in diameter. It also detects skin structures, vascular composition and recticular pigment networks.
SolarScan®	Polartehnics Ltd., Sydney, Australia	The SolarScan compares the features against images of melanomas and non-melanomas in a database and returning an advice to a general physician. It records graphic map of body, but requires oil immersion. It also requires empirical database for comparison, session and image-level accuracy calibration.
Tape Stripping mRNA		This is a simple, fast and painless method for any skin. But it also requires larger gene expression profile for comparison.
Ultrasound Technology		This gives information of inflammatory processes of skin. But it overestimates tumor thickness. The images from this system can be difficult to interpret.

IV. PROCESS OF DIGITAL IMAGE PROCESSING OF SKIN CANCER

As with many computer-aided detection applications, the aim is to detect potentially malignant tumours and lesions in medical images. In most of these algorithms this is done using a three-stage system, viz., identification of potentially unhealthy regions of interest, computation of descriptive features and labelling by a classifier.

In real world applications, it is evident that images not only contain instances of the objects of interest, but also large amounts of background pixels. If no elementary shape features are available for the input data, one has to rely solely on the information provided by color and texture attributes.

The processing consists of extracting the useful and desired information of the melanoma. The shapes corresponding to the globular and recticular pattern and the colors corresponding to the homogenous red/blue/green pigmentation pattern are also detected.

The proposed steps of skin cancer detection and diagnosis are shown in Fig. 2.

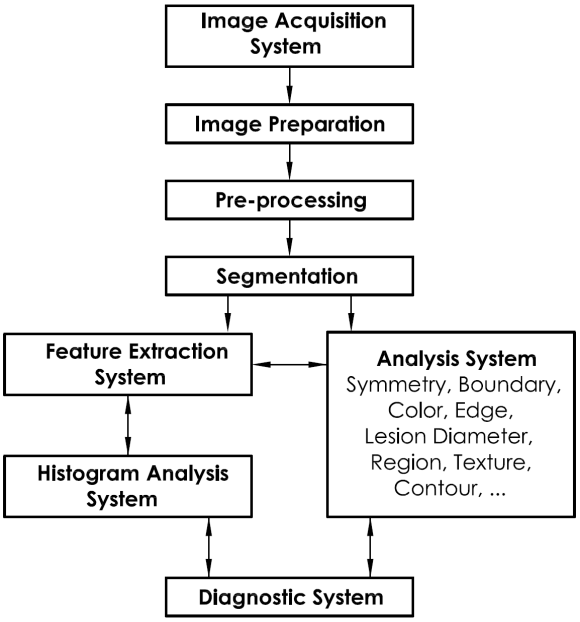

Fig.2 Proposed scheme of skin cancer detection and diagnosis

Step 1 Image acquisition

The first step in skin cancer detection is the skin inspection to find melanoma and in computer aided diagnostic system it involves acquisition of the digital image of affected skin. There are various techniques to acquire skin cancer lesion's image as given below and shown in Fig. 3.

Simple Techniques - Video RBG Camera [19], Still CCD Camera (Specialized or commercially available) [20]

Advanced techniques - Tissue microscopy [21], Epiluminscence microscopy (ELM or Dermoscopy) [22], Transmission electron microscopy (TEM), Video microscopy [23], Ultravoilet illumination [24], Computed tomography (CT), Position emission tomography (PET), MRI

Alternative Techniques - Multi-frequency electrical impedance [25], Raman spectra [10], Side- or Epi-transillumination (using Neviscope) [15].

Mostly ELM or dermoscopy is used for the diagnosis of skin cancer. It uses a hand-held lighted magnifier to analyze skin lesions by observing newly defined and descriptively named subsurface structures (e.g., dots, streaks, veils, networks). Dermoscopes usually facilitate a 10-times magnification of the skin.

But now-a-days CAD is also used by clinicians. Most of the times Clinicians receives or takes noisy images that are degraded by optical lens system in a digital camera. This leads to difficulties in the diagnosis done by visual evaluation, as the information contents of digital images are very complex. Efficient image processing techniques must therefore be developed to help physicians to making a correct and accurate diagnosis.

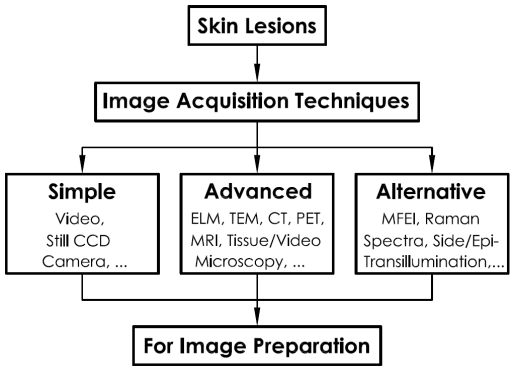

Fig.3 Techniques to acquire skin cancer lesion's digital image

Step 2 Image Pre-processing

Digital images of skin cancer are collected in Bitmap or JPEG format from different sources. Generally indexed images with linear monotonic color maps are used so that RGB images are converted to indexed images. Fig. 4 shows the steps in image preparation. It prepares the image from ordinary image to first RBG then grayscale and at the end binary.

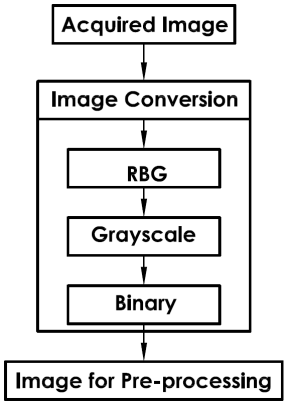

Fig.4 Image Preparation

Image pre-processing makes an acquired-prepared image suitable for a particular application. It basically involves improvement or enhancement of image, which includes noise removal, edge highlighting, sharpening, deblurring, brightening, change in image contrast, masking, hair removal, cropping or resizing as shown in Fig. 5. The pre-processing step removes the undesirable parts, enhances the image, corrects the image skew and removes noise from the image.

In order to detect the border of melanomas, there are numerous techniques (please refer Fig. 5) intended for edge detection. One of the most applicable is the Canny Edge Detection, which firstly smoothes the image to eliminate noise. It then finds the image gradient to highlight regions with high spatial derivatives. The algorithm then tracks along these regions and suppresses any pixel that is no at its maximum (no maximum suppression). The remaining pixels that have not

been suppresses are treated by two thresholds and if the magnitude is below the first threshold, it is set to zero. If the magnitude is above the high threshold, it is made an edge. And if the magnitude is between the two thresholds, then it is set to zero.

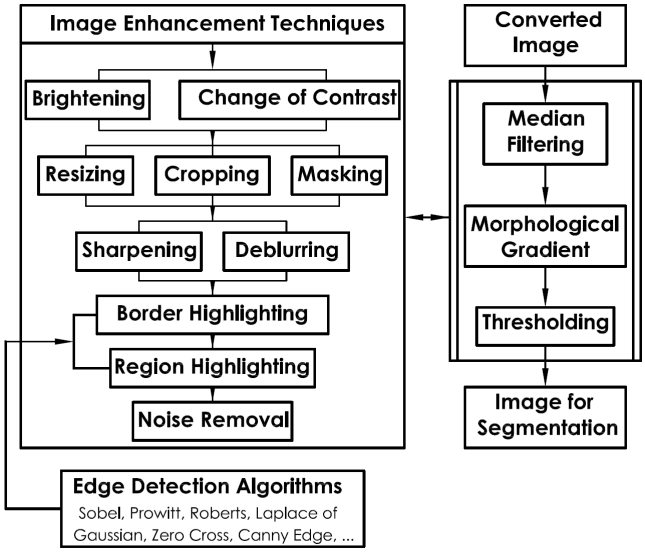

Fig.5 Image Pre-processing

Hair is one of the most undesirable elements that are sometimes present in acquired images. While blond hair can be left without problem, the dark hairs must be masked out in the image processing schemes. Therefore, the image pixels belonging to hair must be replaced by values obtained with some interpolation technique.

Step 3 Image Segmentation

It is a process of image partitioning into multiple segments or regions or structures of interest, so that the contents of each region have similar characteristics. It is a process of extracting and representing information from the image to group pixels together with region of similarity.

Changing the image representation into a meaningful and easy-to-analyze one is the primary aim of segmentation. In a given image, it assigns a label to each pixel, such that pixels with same labels share common visual characteristics. It makes an image processing tasks easier for analysis. Image segmentation is used to locate objects and boundaries in improved images. Image segmentation results in a set of regions that collectively cover the entire image or set of contours extracted from the images.

Images are scanned from top-left to bottom-right and from bottom-right to top-left. During each scan, unique labels are assigned to each detected regional minima.

A segmentation method is usually designed taking into consideration the properties of a particular class of images. A three-step segmentation method using the properties of skin cancer images is as follows:

1. Pre-processing - A color image is transformed into an intensity image in such a way that the intensity at a pixel shows the color distance of that pixel with the color of the background. The color of the background is taken to be the median color of pixels in small windows in the four corners of the image.
2. Initial segmentation - A threshold value is determined from the average intensity of high gradient pixels in the obtained intensity image. This threshold value is used to decide approximate lesion boundaries.
3. Region refinement - A region boundary is refined using edge information in the image. This involves initializing a closed elastic curve at the approximate boundary, and shrinking and expanding it to fit to the edges in its neighborhood.

Step 2 and 3 are shown as Image Post-processing in Fig. 6. There are many image segmentation techniques, such as, threshold based segmentation, edge based segmentation, region based segmentation, clustering based image segmentation, markov random field based segmentation or hybrid segmentation techniques, used in image processing.

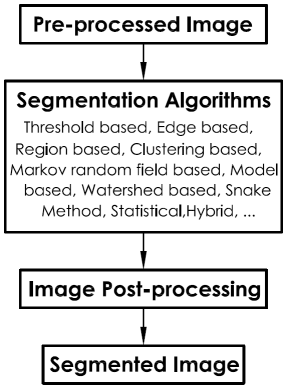

Fig.6 Image Segmentation Process

Step 4 Feature Extraction

Feature extraction is a sub-division of improved image into constituent parts or isolation of some aspects of an image for identifying or interpreting meaningful object forms, which includes finding lines, circles or specific shapes and identifying pimples, white heads or black heads, etc.

The segmented image is further used to extract features such as texture, color and shape. Some of important properties (or descriptors) of the texture are coarseness, smoothness, regularity, of the color are light rate, medium rate, dark rate, while the common shape descriptors are length, breadth, aspect ratio, area, location, parameter, compactness, etc.

The steps in feature extraction process are shown in Fig. 7. But unfortunately, the feature extraction is often subject to error.

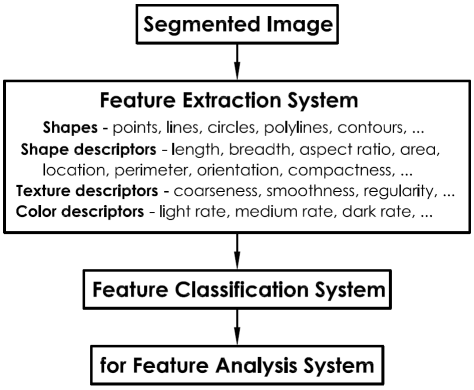

Fig.7 Feature Extraction Process

Then the segmented image is classified based on the extracted features, viz. the texture and color. The design of classifiers were investigated in many studies, most of them being Artificial Neural Networks. Some applied a hard threshold to the histogram of the red/blue/green color component in order to obtain the lesion boundary. Very simple parameters, such as area and perimeter, are extracted. Some measurements on the different color components are also used, and the lesion is once more detected using a global thresholding technique. Some of them try to critically examine image analysis techniques. However, they use very simple feature extraction methods, such as the principal component of a binary mask of the lesion to quantify asymmetry

Texture Classification - The textures are represented by texels. The identification of specific textures in an image is done by modeling texture as a two-dimensional (2D) gray level variation. By estimating degree of contrast, regularity, coarseness and directionality, the relative brightness of pixels are computed.

Color pattern Classification - It is based on the color matching in the segmented image. The computation of a color histogram from segmented image is the most important step to identify the proportions of pixels within an image which holds specific values that we humans express as colors. Color examination does not depend on image size or its orientation and color classification normally involves comparison of color histograms.

Step 5 Feature Analysis

Image analysis techniques involves the measurement of extracted image features. Measurement of image features for diagnosis of melanoma requires that first, the lesions be detected and localized in an image. It is essential that lesion boundaries are determined accurately so that measurements, e.g. maximum diameter, asymmetry, irregularity of the boundary, and color characteristics can be accurately computed.

Textural Analysis is the attempt to quantify texture notions such as “fine,” “rough” and “irregular” and identify, measure and utilize the differences between them. Textural features and textural analysis methods can be loosely divided into two categories, viz., statistical and structural. Statistical methods define texture in terms of local gray-level statistics that are constant or slowly varying over a textured region. Different textures can be discriminated by comparing the statistics computed over different sub-regions. Some of the most common textural features are, neighboring gray-level dependence matrix, dissimilarity, angular second moment, GLCM standard deviation.

Step 6 Histographic Analysis

Wavelet analysis is used for decomposing the skin lesion image and utilizing wavelet coefficients for its characterization. Wavelets are an extension Fourier analysis. Wavelets are a mathematical tool for hierarchically decomposing functions in the frequency domain by preserving the spatial domain. This property can be exploited to segment objects in noisy images based on their frequency response in various frequency bands, separating them from the background and from other objects. The major advantage of using wavelets is that they can be used for analyzing functions at various scales. It stores versions of an image at various resolutions, which is very similar how the human eye works.

In practical applications for various medical imaging systems, features of interest and noise properties have significantly different characteristics. These properties can be efficiently and separately characterized with the techniques of Wavelet Decomposition. The steps required to compress an image using Wavelet transform are as follows:

i. Digitize the source image into a signal which is a string of numbers.
ii. Decompose the signal into sequence of wavelet coefficient w.
iii. Use threshold to modify wavelet coefficient w1 to another coefficient w2.

Wavelet packets provide more flexibility on partitioning the spatial-frequency domain, and therefore improve the separation of noise and signal into different sub-bands in an approximated sense (this is referred to the near diagonalization of signal and noise). In numerical analysis and functional analysis, a Discrete Wavelet Transform (DWT) is any wavelet transform for which the wavelets are discretely sampled. As with other wavelet transforms, a key advantage it has over Fourier transforms is temporal resolution - it captures both frequency and location information (location in time).

A 2D wavelet transform is needed to analyze 2D signals like images. However, separable 2D transform can be

implemented using series of two 1D transforms. As an example, two dimensions DWT of images is implemented by applying 1D transforms on rows of the image, followed by columns transform applied to transformed row. One level 2D discrete wavelet decomposition and Reconstruction implemented using filter banks is explained in the Fig. 8.

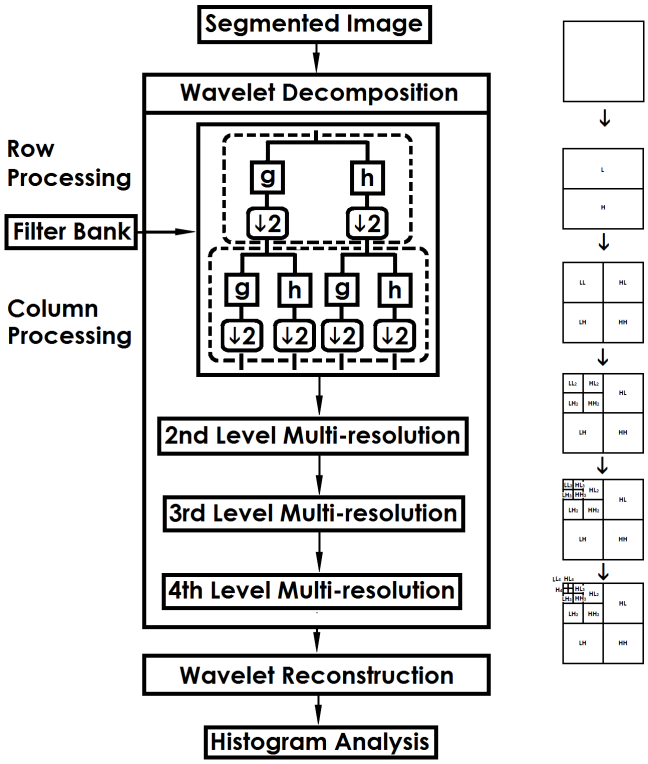

Fig.8 Histographic Analysis using Multi-level Wavelet Decomposition and Transformation

Wavelets decompose an image into orthogonal sub bands with low–low (LL), low–high (LH), high–low (HL), and high–high (HH) components which correspond to approximation, horizontal, vertical and diagonal respectively. The LL sub-band is further decomposed into another four sub-bands; horizontal, vertical and diagonal respectively. The LL sub-band is further decomposed into another four sub-bands; and the Low–low–low–low (LLLL) component, which represents the image approximation at this level, is decomposed once again.

In the next stage, we can perform multi-level (upto 4^{th} level) multi-resolution 2D wavelet decomposition on the input image. Next, we reconstruct the image by using reconstruction function, which computes the matrix of reconstructed coefficients of level N, based on the wavelet decomposition Structure. We can also compute Single-level inverse discrete 2D wavelet transform by using the inverse function. After getting the reconstructed image, we will smooth the image by using different windowing filtering techniques. We can also convert the processed image into binary image for further analysis.

Step7 Skin health Diagnosis System

Skin Health Diagnosis is a process of identifying a skin texture or problem by its signs, symptoms. Diagnosis system is a system that can be used to analyze any problem by answering some questions that lead to a solution to the problem. When melanomas occur, they usually arise from pigmented nevi (moles) that are large (diameter > 6mm), asymmetric, with irregular borders and coloration. Bleeding, itching and a mass under skin are other signs of cancerous change.

As in the traditional visual diagnosis procedure, the computer-based systems must looks for features and combine them to characterize the lesion as benign or malignant melanoma. The features must be measurable and must have high sensitivity and high specificity.

Several different algorithms for skin cancer diagnosis are used worldwide to differentiate melanoma from benign melanocytic lesions. They are

1. Pattern Analysis
2. ABCD(E) rule of dermoscopy
3. 7-point checklist
4. CASH
5. Menzies method

Pattern Analysis/Recognition

Historically pattern recognition has been used to differentiate benign from malignant neoplasm by clinicians. It was described by Pehamberger, H. [26]. Pattern analysis techniques have been widely applied to analysis and recognition of cancer, evaluation of the effectiveness of treatment and prediction of the development of cancer. This method is used to identify specific patterns, which may be global (recticular, globular, cobblestone, homogeneous, starburst, parallel, multi-component, nonspecific, atypical vessels, etc) or local (pigment network, dots/globules/moles, streaks, blue-whitish veil, regression structures, hypo-pigmentation, blotches, vascular structures) and color (Homogeneous blue pigmentation, Patch of pigment, Blue-Gray points, Blue-White Veil) can be present in melanocytic tumors. The location and distribution of shapes and colors can often create different visual patterns that are characteristic of certain lesions.

In the first stage, the dermatologist must decide, whether or not the lesion is melanocytic? This classification helps to correctly classify a lesion as a melanocytic tumor, spleen cell carcinoma, hemangioma, seborrheic keratosis or dermatofibroma. When a skin lesion does not meet any of the criteria, the tumor is considered to be of melanocytic origin. In presence of few criteria, it is considered as a potential melanoma, especially when there are irregular or pinpoint vessels. And with a tumor of melanocytic lesion criteria, the dermatologist proceeds, to the second stage to differentiate between a benign lesion (melanocytic nevi) and melanoma.

Pattern matching & Artificial Neural Networks technique presents difficulties in detecting shapes inside a melanoma due to the unpredictable reduced similarity that exists between samples and the randomness of the patterns, in comparison with the predictable structure of faces and the tardiness in producing a result.

ABCD(E) Rule

It is one of the easiest guides to the most common signs of melanoma. In 1985, recognizing the need to educate physicians and the public to recognize melanoma in its early clinical presentation, group from New York University [18] devised the ABCD acronym (Asymmetry, Border irregularity, Color variegation, Diameter > 6mm). Stolz, W. [27] established this diagnosis scheme for dermatoscopic images known as the ABCD rule of dermatoscopy. The characteristics needed to diagnose a melanoma as malignant are shown in Fig. 9 and explained as

(A) Asymmetry - one half does not match the other. Symmetry or asymmetry in zero, one, or two orthogonal axes are considered. Also color, texture, and shape must be taken into account.
(B) Border irregularity - the edges are ragger, notched or blurred. The lesion is divided into eight radial pieces which are then labeled as showing a sharp cut-off with the surrounding skin or not.
(C) Color - the pigmentation is not uniform. The presence of up to six known colors must be detected - white, red, light brown, dark brown, slate blue, and black.
(D) Diameter - the width is greater than 6mm. Differential structures with at least five patterns are relevant for specific types of lesions. Any growth of a mole should be of concern.

Some melanomas do not fit the ABCD rule described above, so it is important for us to notice changes in skin markings or new spots on our skin.

The need to recognize lesion change is added with “E” for “Evolving,” in our acronym ABCD, which substantially enhanced the ability of physicians and laypersons to recognize melanomas at earlier stages. “E” for Evolving is especially important for the diagnosis of nodular melanomas, which frequently present as smaller lesions at more advanced stages (i.e., thicker tumors) where early recognition is even more crucial. ABCDE is a simple and strongest tool which had demonstrated its effectiveness in the detection of key features of melanoma, including lesion change, in the public domain.

The ABCD(E) rule shows the weakness of the analysis done by physicians. The clinical diagnosis of melanoma could be difficult for a general practitioner and, in some cases, for dermatologists. To enhance and support the clinical evaluation of pigmented skin lesions a computer-aided diagnosis has been introduced. Melanoma recognition is generally easy where the clinical ABCDE rule is applied.

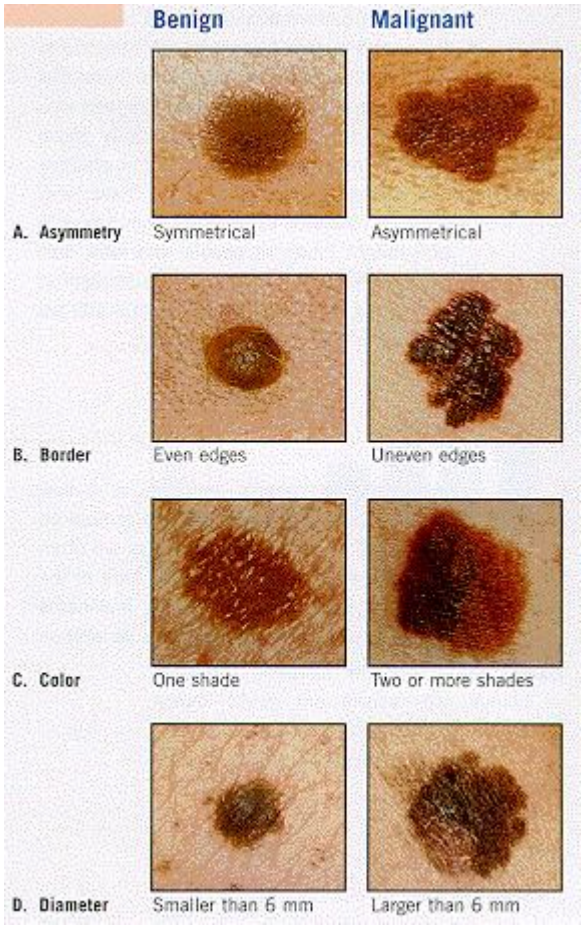

Fig.9 ABCD Rule for detection of Benign or Malignant Skin Cancer [www.metrohealth.org] [28]

The only disadvantage of an automated ABCD rule is that, it provides a less accurate diagnosis because the characteristics analyzed can be present in benign lesions causing a high number of false positives.

Glasgow Seven-point checklist

This method has seven criteria that assess the chromatic characteristics and the shape and/or texture of the lesion as described by Argenziano, G. [29]. This includes 3 major and 4 minor criteria. The major criterion includes change in size, shape and color. They are atypical pigment network, blue-whitish veil, and atypical vascular pattern. The minor criteria includes sensory change, diameter of 7mm or greater and the presence of inflammation, crusting or bleeding. They are irregular streaks, irregular pigmentation, irregular dots/globules, irregular blotches and regression structures. The acquired image of the melanocytic skin lesion is analyzed in order to evidence the presence of these standard criteria; finally, a classified as malignant or nevus.

Due to complex nature of criterion, as compared with ABCD(E) criteria, the Glasgow checklist has been less widely adopted.

CASH

To differentiate benign with that of malignant melanocytic lesions, appearance of color(C), architectural order (A), symmetry of pattern (S) and homogeneity (H) are important considerations [30]. Benign melanocytic lesions have few colors, architectural order, symmetry of pattern or homogeneity whereas malignant melanoma has many colors, architectural disorders, asymmetry of pattern and heterogeneity.

Menzies Method

This method is used to identify negative features (symmetry of pattern, presence of a single colour) and positive features (blue-white veil, multiple brown dots, pseudopods, radial streaming, scar-like depigmentation, peripheral black dots/globules, multiple (five to six) colors, multiple blue/gray dots, broaden network). This method is considerably complex and explained by Menzies, S. W. [31].

Studies have demonstrated the usefulness of the ABCD paradigm in enhancing early melanoma diagnosis as a part of clinical examinations. We are using ABCD criteria in the digital image analysis's diagnostic system, as it has proven more accurate and effectiveness in clinical practice as shown in Table III

TABLE III
COMPARISON OF DIAGNOSTIC ACCURACY OF DERMOSCOPY ALGORITHMS

Sr.	Diagnostic Algorithm	Diagnostic Accuracy
1	Pattern Analysis [32]	71%
2	ABCD [32]	76%
3	7-point checklist [32]	58%
4	CASH [30]	-
5	Menzies [31]	81%

The ABCD(E) rule is also used by the American Cancer Society, American Academy of Dermatology and others and have been featured in the lay press to provide simple parameters for evaluation and identification of pigmented lesions that may need further examination. But all melanomas do not have all four ABCD features. It is the combination of features (e.g., A+B, A+C, B+C, A+B+C, etc.) that render cutaneous lesions most suspicious for early melanoma.

The complete process illustration of diagnostic system is shown in Fig. 10.

Decision System

A skin classifier defines a decision boundary of the skin color class in color space based on a fuzzified skin-colored pixels & severity of cancerous cell. Skin classifier defines a decision boundary of the skin color class in a feature space. The feature space is the color space chosen. The choice of the skin classifier is influenced by the shape of the skin class in the color space chosen by a skin detector.

The Fuzzy inference is the process of formulating the mapping from a given input to an output using fuzzy logic. In the Fuzzy Inference System, skin color as input variable is fuzzified by applying membership function to it. We divide color of skin as Light Red, Medium Red and Dark Red as linguistic variable. Similarly output variable are based on the fuzzy-based Madmani, having status as healthy skin, rash skin, cancer skin. The mapping then provides a basis from which decisions can be made. The process of fuzzy inference involves all of the pieces that are described in Membership function's logical operations and If-then rules.

The rules are set in human language as given below:
Rule1: If "skin color" (input variable) is Light Red then decision (output variable) Healthy skin.
Rule 2: If "skin color" (input variable) is Medium Red then decision (output variable) is Rash skin.
Rule 3: If "skin color" (input variable) is Dark Red then decision (output variable) is Cancer skin

Complete diagnosis is proposed to be implemented in MATLAB® fuzzy inference system.

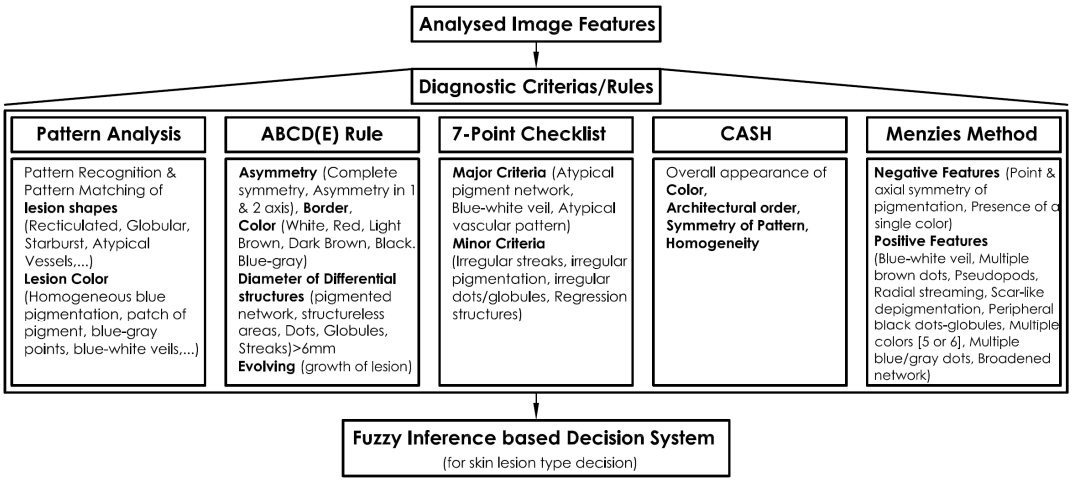

Fig.10 Process Illustration of Diagnostic System

V. Proposed Automated Skin Cancer Diagnosis Algorithm using Wavelets and Fuzzy Inference System

1. Skin lesion image is acquired using dermatoscope or commercially available digital camera.

2. Convert acquired image from RBG to GrayScale image and then to binary - Conversion of RBG to grayscale image reduces the memory consumption & decreases the processing time. The grayscale conversion is done by summing the values of every pixels of the red, blue and green layer of the color image as given in Eq.1. Since the result may be higher than 256, the entire resulting matrix should be normalized. Thus the higher value will always be 256.

$$I_{GS}(x,y)=\frac{1}{3}\left[\sum_{z=1}^{3} I_{RBG}(x,y,z)\right] \qquad \text{Eq.1}$$

$I_{GS}(x,y)$ is the Grayscale image and $I_{RBG}(x,y,z$ is the RBG image.

3. Correction of RBG image of 64×64 pixels (contrast, brightness, etc).

4. Shape/Edge Detection - Canny Edge Detection algorithm is applied to the grayscale image (not blurred). The edges are represented as white pixels (value '1') in binary image of the same size as the original image. The process is

i. Convolve the image with the derivative of a Gaussian.
ii. Apply non-maximal suppression to the gradient magnitude image.
iii. Use two thresholds $\tau_1 > \tau_2$:

$$\text{(a) Class} = \begin{Bmatrix} \text{edge if magnitude} > \tau_1 \\ \text{candidate if magnitude} > \tau_2 \end{Bmatrix} \qquad \text{Eq.2}$$

(b) Hysteresis - any candidate which is a neighbour, in the gradient direction, of the edge is reclassified as an edge.

5. As it has been mentioned above, blurring the grayscale image had the aim of smoothing the border for a better region detection of the skin lesion. The shape extraction is a key stage for reducing the false positive rates, because it prevents the processing of different forms that do not belong to the skin lesion.

$$I_{BI}(i,j)=\begin{Bmatrix} 1 \rightarrow I_{BGS}(i,j) < mean(I_{GS}) \\ 0 \rightarrow else \end{Bmatrix} \qquad \text{Eq.3}$$

$I_{BGS}(i,j)$ is the blurred grayscale image and $I_{BI}(i,j)$ the binary image.

6. In order to extract the shape, the mean value of the image is calculated and those pixels that have a value below the mean will be assigned a white pixel on the binary image. As a consequence, the skin lesion's region will be represented with white and the outside with black (values '1' and '0' respectively). The pixels that are darker than the mean of the image are a considered part of the melanoma. The shape is placed on a binary image where the white corresponds to the region.

7. Skin lesion image shape/region extraction - For this extraction image should be filtered (low pass). Gaussian blur is applied to reduce the image sharpness, so that border of the detected region is smoothen. The Gaussian blur is defined in Eq. 3. The Gaussian blur is a type of image-blurring filters that uses a Gaussian function (which also expresses the normal distribution in statistics) for calculating the transformation to apply to each pixel in the image.

$$I_F(x,y)=C_K(k,l)\otimes I_{RBG}(x,y)=\sum_{k=-N}^{N}\sum_{l=-N}^{N} C_K(k,l).I[(x-k),(y-l)] \qquad \text{Eq.4}$$

where $C_K(k,l)$ is the convolution kernel, $I_{RBG}(x,y)$ is the original image, $I_F(x,y)$ is the filtered image and 2N1 is the size of the convolution kernel.

When applied in two-dimensions, above formulae produces a surface whose contours are concentric circles with a Gaussian distribution from the center point. Values from this distribution are used to build a convolution matrix that is applied to the original image. Each pixel's new value is set to a weighted average of that pixel's neighborhood. The original pixel's value receives the heaviest weight (having the highest Gaussian value) and neighboring pixels receive smaller weights as their distance to the original pixel increases. This results in a blur that preserves boundaries and edges better than the other, more uniform blurring filters.

8. Removal of Unwanted Information from Grayscale Image - Now that the edge has been detected and the region of the lesion has been extracted, the next step is to remove all the information that does not belong to the inside of this region. The reason for this is to avoid unnecessary processing and false positive detection of shapes. An overlay between the input image and the binary image takes place I order to remove color from outside the area of the skin lesion.

$$I(x,y)=I_{ED}(x,y)\times I_{SH}(x,y) \qquad \text{Eq.5}$$

$I_{ED}(x,y)$ is the image containing the edges, $I_{SH}(x,y)$ is the image containing the shape of the skin lesion and $I(x,y)$ is the resulting image with information only from the inside of the lesion.

When the images $I_{ED}(x,y)$ and $I_{SH}(x,y)$ are multiplied pixel by pixel, the black pixels (value '0') delete the edges that are outside the region of the lesion. To delete this unwanted information, the binary image containing the edges and the image containing the shape of the skin lesion are multiplied in order to delete the information from outside the skin lesion using Eq. 5.

9. Removal of Unwanted Information from RBG Image - To delete unwanted information, the RBG image and the image containing the shape of the skin lesion are multiplied in order to delete the information from outside the skin lesion, using Eq. 6, but applied to the red, blue and green layers.

$$I_{CL}(x,y)=I_{RBG}(x,y)\times I_{SH}(x,y) \qquad \text{Eq.6}$$

$I_{RBG}(x,y)$ is the RBG image, $I_{SH}(x,y)$ is the image containing the shape of the skin lesion and is the resulting

color image with information only from the inside of the lesion.

10. The image is separated in three RBG layers. A summation of each column of each RBG layer is stored in one array per layer as shown in Eq. 7.

$$V_{CL}(j) = \sum_{i=1}^{64} \mathrm{I}_{CL}(i, j) \qquad \text{Eq.7}$$

$\mathrm{I}_{CL}(i, j)$ is the image containing only information from the inside of the lesion and is the array containing the values of color (red, blue or green) in each column of the images.

11. Each array is normalized for 256 bits as shown in Eq. 8.

$$V_{CL}^{'}(j) = \frac{V_{CL}(j)}{V_{CL}MAX} \qquad \text{Eq.8}$$

$V_{CL}(j)$ is the array containing the values of color (red, blue or green) in each column of the above image and is the normalized color array.

12. Since the summation of the same pixel from the three RBG layers can lead to situation due to the lack of bits to represent that intensity, the resulting matrix should be normalized to 256.

The values of each array are represented in $255 \times 64 \times 1$ matrixes where the height corresponds to the value of each position of the array as shown in Eq. 9.

$$C_{\mathrm{I}}\left[V_{CL}^{'}(j), j\right] = 1 \qquad \text{Eq.9}$$

$V_{CL}^{'}(j)$ is the normalized color array and C_{I} is the matrix containing the intensity of color per column. C_{I} are three matrices (one per each RBG color) that represent the intensity of a specific color in each column of the image. After the creation of $C_{\mathrm{I}-RED}$, $C_{\mathrm{I}-BLUE}$ and $C_{\mathrm{I}-GREEN}$, the three matrixes are assembled in one RBG image.

13. The image is horizontally split in an upper and lower half. Then, the mean value of each layer of the upper part is calculated.

14. Finally, the percentage of red, blue and green is calculated using Eq. 10abc.

$$\mathrm{Re}\,d(\%) = \frac{\mathrm{Re}\,d}{Blue + Green} \times 100 \qquad \text{Eq.10a}$$

$$Blue(\%) = \frac{Blue}{\mathrm{Re}\,d + Green} \times 100 \qquad \text{Eq.10b}$$

$$Green(\%) = \frac{Green}{Blue + \mathrm{Re}\,d} \times 100 \qquad \text{Eq.10c}$$

Red /Blue/Green are the number of red /blue/green pixels respectively.

15. The number of value '1' in the upper halves of $C_{\mathrm{I}-RED}$, $C_{\mathrm{I}-BLUE}$ and $C_{\mathrm{I}-GREEN}$ is calculated in order to determine if the red/blue/green pixels predominate over other two. If so, the lesion presents red/blue/green pigmentation respectively.

16. Wavelet Transformation, Decomposition, Reconstruction - The wavelet is represented as

$$W(j) = W(j+1) \oplus U(j+1) \qquad \text{Eq.11}$$

where $U(j+1)$ is orthogonal complement subspace of $W(j)$ in $W(j+1)$.

The discrete wavelet transformation of a given image signal is further processed in wavelet decomposition which involves extraction of coarser approximation and detail signals from approximate signal to next level of finer multi-resolution stage. The reconstruction of approximation signal from approximate and details of coarser Subspace is given as

$$C(j,k) = \sum_{N} g(k-2N)C(j+1,N) + \sum_{N} h(k-2N)D(j+1,N) \qquad \text{Eq.12}$$

Where $C(j,k)$ is the input image signal, $g(k-2N)$ & $h(k-2N)$ are filters and $C(j+1,N)$ & $D(j+1,N)$ are coarser approximate & detail image signal at that resolution level. Wavelet is also used for image enhancement by denoising the given image.

17. Diagnostic System - ABCD Rule

For the diagnostic system, we are proposing to use ABCD rule. A brief summary is provided of the equations that were used to analyze the **a**symmetry, **b**order, **c**olor and **d**iameter using Eq. 13abcd.

$$\text{Asymmetry factor} = \frac{\sum_{j=1}^{n/180}\left[\frac{P_j}{(T/2)}\right]}{(n/180)} - 1 \qquad \text{Eq.13a}$$

$$\text{Border factor} = \frac{\sum_{j=1}^{n/360}\left[\frac{r_j - r_{MIN}}{r_{MAX} - r_{MIN}}\right]}{(n/360)} \qquad \text{Eq.13b}$$

$$\text{Color factor} = \frac{\sum_{j=1}^{T}\left[\frac{P_j - P_{MIN}}{P_{MAX} - P_{MIN}}\right]}{T} \qquad \text{Eq.13c}$$

$$\text{Diameter} = r_{MAX} \qquad \text{Eq.13d}$$

N is the degree of rotation, P is the value of a pixel, r is the distance between a pixel and the center and T is the number of pixels in the lesion (mole/nevi).

18. Fuzzy Inference Decision System - This will give us quantitative information about ABCD factors which will be further used along with Fuzzy Inference system. We are concentrating on the red color and accordingly we are getting the diagnosis system output as Normal Skin, Rash Skin or Cancer Skin. Furthermore, the analysis result can be used to indicate whether the mole is benign, suspicious or potentially dangerous.

VI. Conclusions

Skin cancer diagnosis system identifies and recognizes skin cancer symptoms and diagnoses melanoma in early stages. A review of skin cancer detection system has been done with the emphasis of the automated Computer Aided Diagnosis (CAD)

of the present day. With the proper image input using different Digital Image Processing steps, doctors can get very good help from such diagnostic systems. We are proposing to use ABCD rule as its diagnostic accuracy has been reported to be 76%. A combination of both ABCD rules and wavelet coefficients has been shown to improve the image feature classification accuracy by 60%. At the end, we proposes algorithm with relevant processing mathematics for proper, efficient detection of skin cancer. We hope that the proposed algorithm will help doctors. This system will save doctor's time and also can be used for regular monitoring skin cancer development in patients. Early diagnosis is more than 90% curable and late is less than 50%.

REFERENCES

[1] www.skincancer.org

[2] Indira, D.N.V.S.L.S. and Jyotsna Suprya, P., "Detection & Analysis of Skin Cancer using Wavelet Techniques," International Journal of Computer Science and Information Technologies, Vol. 2(5), pp.1927-1932, 2011.

[3] Jain, Y. K. and Jain, M., "Comparison between Different Classification Methods with Application to Skin Cancer," International Journal of Computer Applications, Vol. 53, No.11, pp. 18-24, Sept. 2012.

[4] Fatima, R., Khan, Mohd. Z. A., Govardhan, A. and Kashyap, D. D., "Computer Aided Multi-Parameter Extraction System to Aid Early Detection of Skin Cancer Melanoma," International Journal of Computer Science and Network Security, Vol.12, No.10, pp.74-86, Oct. 2012.

[5] Alamelumangai, N. and DeviShree. J., "PSO Aided Neuro Fuzzy Inference System for Ultrasound Image Segmentation," International Journal of Computer Applications, Vol. 7, No.14, pp. 16-20, Oct. 2010.

[6] Fassihi, N., Shanbehzadeh, J., Sarafzadeh, A., and Ghasemi, E., "Melanoma Diagnosis by the Use of Wavelet Analysis based on Morphological Operators," Proc. of International MultiConference of Engineers and Computer Scientists 2011, Vol. I, Hong Kong, pp. 1-4, March 16-18, 2011.

[7] Alcon, J. F., Ciuhu, C., Kate, W. ten, Heinrich, A., Uzunbajakava, N., Krekels, G., Siem, D. and Haan, G. de., "Automatic Imaging System With Decision Support for Inspection of Pigmented Skin Lesions and Melanoma Diagnosis," IEEE Journal of Selected Topics in Signal Processing, Vol. 3, No. 1, Feb. 2009, pp. 14-25.

[8] Jung, C. R., and Scharcanski, J., "Sharpening Dermatological Color Images in the Wavelet Domain," IEEE Journal of Selected Topics in Signal Processing, Vol. 3, No. 1, pp.4-13, Feb. 2009.

[9] Odeh, S. M.,"Using an Adaptive Neuro-Fuzzy Inference System (AnFis) Algorithm for Automatic Diagnosis of Skin Cancer," Journal of Communication and Computer,Vol.8, pp.751-755, 2011.

[10] Sigurdsson, S., Philipsen, P. A., Hansen, L. K., Larsen, J., Gnidecka, M. and Wulf, H. C., "Detection of Skin Cancer by Classification of Raman Spectra," IEEE Trans. on Biomedical Engineering, Vol.51, No.10, pp.1784-1793, Oct. 2004.

[11] Bhattacharyya, S., "A Brief Survey of Color Image Preprocessing and Segmentation Techniques," Journal of Pattern Recognition Research, Vol.1, pp. 120-129, 2011.

[12] Ogorzałek, M. J., Surowak, G., Nowak, L. and Merkwirth, C.., "New Approaches for Computer-Assisted Skin Cancer Diagnosis," The Third International Symposium on Optimization and Systems Biology, Zhangjiajie, China, Sept. 20-22, pp. 65-72, 2009.

[13] Blackledge, J. M. and Dubovitskiy, D. A., "Object Detection and Classification with Applications to Skin Cancer Screening," ISAST Transactions on Intelligent Systems, Vol. 1, No. 2, pp.34-45, 2008.

[14] Silveira, M., Nascimento, J. C., Marques, J. S., Marcel, A. R. S., Mendonça, T., Yamauchi, S., Maeda, J. and Rozeira, J., "Comparison of Segmentation Methods for Melanoma Diagnosis in Dermoscopy Images," IEEE Journal of Selected Topics in Signal Processing, Vol. 3, No. 1, pp.35-45, Feb. 2009.

[15] Patwardhan, S. V., Dhawan, A. P. and Relue, P. A., "Classification of melanoma using tree structured wavelet Transforms," Computer Methods and Programs in Biomedicine, Vol. 72, pp.223-239, 2003.

[16] Day, G. R. and Barbour, R. H., "Automated melanoma diagnosis: where are we at?," Skin Research and Technology, pp.1-5, 2000.

[17] www.emedicinehealth.com

[18] Rigel, D.S., Russak, J. and Friedman, R., "The Evolution of Melanoma Diagnosis: 25 Years Beyond the ABCDs," CA Cancer Journal of Clinicians, No. 60, pp. 301-316, 2010.

[19] Ercal, F., Chawla, A., Stoecker, W.V., Lee, H-C. and Moss, R.H., "Neural network diagnosis of malignant melanoma from color images," IEEE Trans. of Biomedical Engineering, Vol.14, No.9, pp.837-845, Sept. 1994.

[20] Herbin, M., Bon, F., Venot, A., Jeanlouis, F., Dubertret, M., Dubertret, L. and Stauch, G., "Assessment of healing kinetics through the true color image processing," IEEE Trans. of Medical Imaging, Vol.12, No.1, pp.39-43, May 1993.

[21] Sanders, J., Goldstein, B., Leotta, D. and Richards, K., "Image processing techniques for quantitative analysis of skin structures," Computational Methods and Programming in Biomedical, Vol.59, pp.167-180, 1999.

[22] Ganster, H., Pinz, P., Rohrer, R., Wildling, E., Binder, M., Kittler, H., "Automated melanoma recognition," IEEE Trans. of Medical Imaging, Vol.20, No.3, pp.233-239, Mar. 2001.

[23] Grana, C., Pellacani, G., Cucchiara, R., Seidenari, S., "A new algorithms for border description of polarized light surface microscopic images of pigmented skin lesions," IEEE Trans. of Medical Imaging, Vol.22, No.8, pp.959-964, Aug. 2003.

[24] Chwirot, B. W., Chwirot, S., Redziski, J. and Michniewicz, Z., "Detection of melanomas by digital imaging of spectrally resolved ultraviolet light-induced autofluorescence of human skin," European Journal of Cancer, Vol.34, pp.1730-1734, Oct. 1998.

[25] Aberg, P., Nicander, I., Hansson, J., Geladi, P., Homgren, U., and Ollmar, S., "Skin cancer identification using multifrequency electrical impedance – A potential screening tool," IEEE Trans. of Biomedical Engineering, Vol.51, No.12, pp.2097-2102, Dec. 2004.

[26] Pehamberger, H., Steiner, A., Wolff, K., "In vivo epiluminescence microscopy of pigmented skin lesions. I. Pattern analysis of pigmented skin lesions," Journal American Academy of Dermatology, No. 17, pp.571-583, 1987.

[27] Stolz, W., Riemann, A., Cognetta, A.B., Pillet, L., Abmayr, W., Holzel, D., "ABCD rule of Dermatoscopy: a new practical method for early recognition of malignant melanoma," European Journal of Dermatology, No.4, pp.521-527, 1994.

[28] www.metrohealth.org

[29] Argenziano, G., Fabbrocini, G., Carli, P., De Giorgi, V., Sammarco, E, Delfino, M., "Epiluminescence microscopy for the diagnosis of doubtful melanocytic skin lesions. Comparison of the ABCD rule of dermatoscopy and a new 7-point checklist based on pattern analysis," Arch. Dermatology, No.134, pp. 1563-1570, 1988.

[30] Henning, J. S., Dusza, S. W., Wang, S. Q., "The CASH (color, architecture, symmetry and homogeneity) algorithm for dermoscopy," Journal of American Academy of Dermatology, No. 56, pp. 45-52, 2007.

[31] Menzies, S.W., Crotty, K.A., Ingvar, C., McCarthy W.H., "An atlas of surface microscopy of pigmented skin lesions," McGraw-Hill Book Company, Sydney, 2003.

[32] Annessi, G., Bono, R., Sampogna, F., Faraggiana, T., Abeni, D., "Sensitivity, specificity and diagnostic accuracy of three dermoscopic algorithmic methods in the diagnosis of doubtful melanocytic lesions: the importance of light brown structureless areas in differentiating atypical melanocytic nevi from thin melanomas," Journal of American Academy of Dermatology, No. 56, pp. 759-767, 2007.